Research Journal of Engineering & Technology. Vol., 1 (2), 74-86, 2024
Available online at http://www.rjetjournal.com
ISSN 2149-3340 ©2024

An Analysis on a Kind of Axial Induced Draft Fan (ID Fan) to Verify Its Performance versus Retrofitting Fan Blades

Mohammadreza Akbari

Lecturer of Mechanical Engineering Department of BONYAN Institute- Esfahan-Iran

*Corresponding Author Email: Akbari.gh.m.r@gmail.com

Abstract: Today we are dealing with a variety of turbo machines. In the current century, we are interested in productivity in order to find out more about the efficiency, flow rate, pressure, temperature and parameters affecting turbo machinery performance. Any changes to the parameters affecting turbo machinery performance affect the operation of turbo machinery and should be analyzed. In the present paper, it is tried to solve the numerical solution of the flue gas from an Induced Draft Fan (ID Fan) which is fractured in blades after period of time. For retrofit blades, several kind of support is considered and performance variation has been reviewed. For this purpose, FLUENT software has been used. In this simulation, the fan is analyzed in 3D. A rotating reference algorithm is used to model rotor rotation. For rotor rotation, the moving boundary condition with zero rotational speed rather Than reference is used. Shell boundary condition is wall condition with non-slip condition. During the simulation, the standard K-ε method has been used. The results show that the supports have a negative effect on fan performance but the cost of repair and replacement is reduced and can be used as a new design.

Keywords: turbo machine, Induced Draft Fan, CFD, Flue gas, Rotating reference algorithm, Non-slip condition, 3D Analysis, Standard K-ε Method

Introduction

Fans are widely used in industrial and commercial applications, which can be used to ventilate a store or the entrance of the air into a combustion chamber or remove combustion products of furnace of a power plant. The fans are used to change the flow pressure in the gas phase to compensate for the system pressure drop. Of course, blowers and compressors are also used to change the pressure. To differentiate between these devices, the pressure parameter itself is usually used. For example, according to ASME, the ratio of the output pressure to input pressure is used to identify the type of turbomachinery. Table (1) is taken from this standard.

Table 1. Comparison of fan, compressor and blower (ASME STANDARD, 2008).

Equipment	*Special ratio*	*Increase in pressure (millimeters of water)*
Fan	1.11	1136
Blower	1.11 till 1.20	1136-2066
Compressor	More than 1.20	-

The two main categories of fans include centrifugal fans and axial fans (Tabatabaee, 2003). The axial fan has three categories, which are: 1) Propeller, 2) Tube axial and 3) Vane axial. The first group is without a duct, the second group has a duct, and the third group has a duct and stationary guide blades in the input and output of the duct (Hadizade, 2015). One-stage axial fans are generally used in power plants to operate as forced draft fans and induced draft fans. The induced draft fans are inserted between air heaters (kind of heat exchanger) and chimney. These fans exhaust the flue gas in the pressure of the atmosphere and place the entire path under negative pressure. These fans should be able to handle corrosive combustion products and ash (EL-Wakill, 1985). When these fans are used to control pressure and flow rate, and they must be responsive to their changes in different situations, they must be equipped with tools for doing so. In centrifugal fans, this is done by the inlet damper, outlet damper, control damper which is exactly at the entrance of the fan, or variable speed fan provides. In axial fans, the flow control is controlled by the blade pitch (Rotating fan blades and variations in blade angles). But control with control damper is also common (U.S Department of Energy). Figure (1) shows a variety of flow control devices and how the flow changes with the power consumption ratio. Each fan has its own characteristic charts according to its type of performance. Figure (2) shows the characteristic diagram of a typical axial fan. Also, various components of an axial fan are shown in Figure 3.

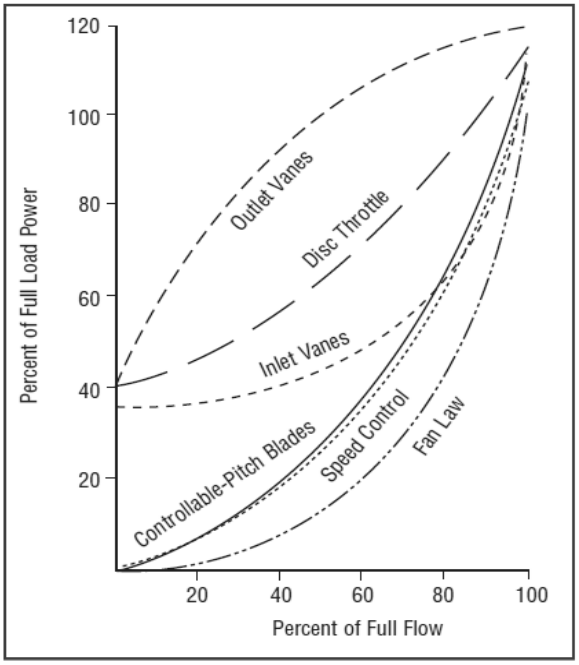

Figure 1. Flow rate versus power for flow control and pressure equipment (U.S Department Of Energy).

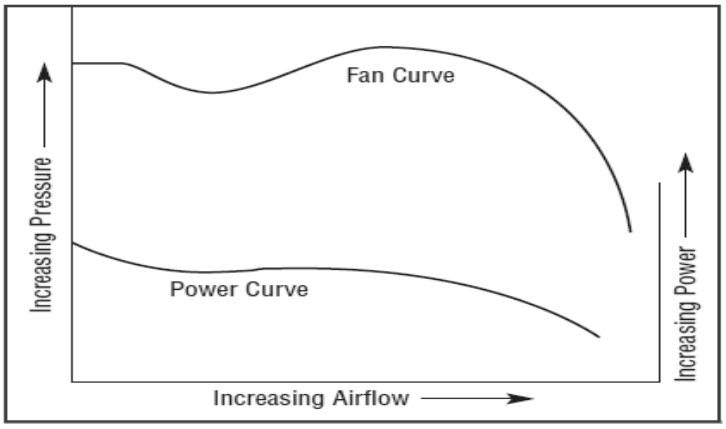

Figure 2. Schematic diagram of an axial fan characteristic (McPherson, 1993).

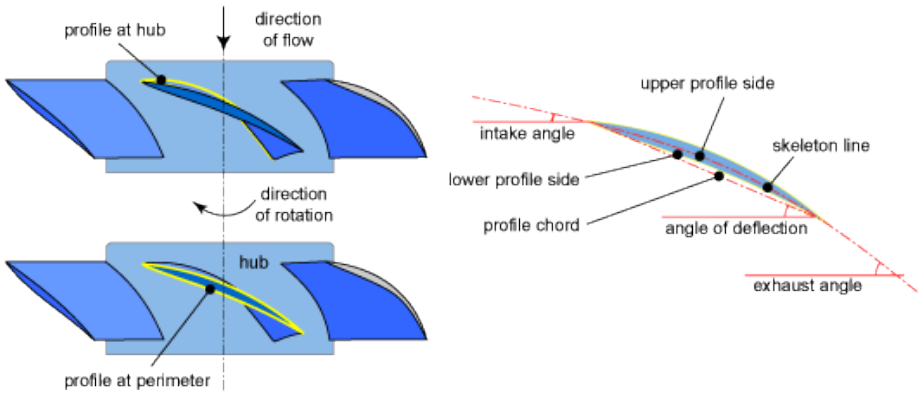

Figure 3. Different components of an axial fan.

In this current study, a kind of induced draft fan is analyzed by computational fluid dynamics (CFD) method. One of the most powerful software in this domain is FLUENT. This software has recently been purchased by ANSYS. And in this article, ANSYS WORKBENCH is used, which has fluent as one of the branches of this software (Akbari & dadkhah, 2017).

Familiarity with analyzed induced draft fan

Shahid Mohammad Montazeri Power Plant boiler with name TME206 / CO is under vacuum type and in order to exhaust of smokes, there are two parallel induced draft fans in each side of these boiler. The output power of Montazeri plant is 200 MW and the problem with the bad performance of one of the fans will be as follows:

1) Disruptions in the work of a fan reduce the output power to 100 MW. (The nominal output of each unit is 200MW)

2) Emergency shot down of one of the fans cause increasing consumption electricity current in other fan and tripping the other fan with overload relay and unit breaking from electricity network by interlocks.

Pay attention to the fact that repair during unit work are faced with different costs and in addition to the cost of repairs and financial losses, costs of again start up comes into existence. Therefore, it will be necessary to study the performance of the fans and optimize them.

These power plant's fans are made by East Germany and during the work and specially during work with fuel oil, because of sitting the soot on blades, unbalances occurs in the fan and when they are working, they encounter with vibration and shake. Sometimes failure occurs in blades, and unbalances increase dramatically and Causing serious damage to other parts of the fan. A sample of this incident is presented in Fig. 4. Different ideas may exist to prevent fractures and even from the company, a type of support in the form of a cane for each blade has been proposed. Figure (5) shows an overview of these fan-mounted cane like supports. It is worth mentioning that the reinforcement of the blades by welds the cane like supports has significantly reduced the number of failures but the problem of blade failure still exists because vibration analyzes on the fans show that the working frequencies of the fan are very close to the fan natural frequencies. The coast down diagram of one of these fans is shown in Fig. 6. The electromotor of this fan works at 740 rpm and 990 rpm. The coast down diagram shows that the critical speed is 730 rpm and 1000 rpm (with outsourcing), which is very close to the fan's speed. Of course, after the implementation of cane like support, increasing the fan's ampere consumption is experienced that this issue shows that only the attention to the endurance of materials and structures will not solve the problem and paying attention to flow rate and performance of the fan need to be examined after retrofitting with different supports. For analyze the fan's flow rate and path lines, the fan is simulated with and without supports. After initial simulation and verifying the results with the catalog values, for new manners, fan is simulated. It has also been tried to review the company's recommendation and new designs to be presented. The flow rate of fan according to the manufacturer's catalog in the nominal load is given in Table (3) that is for 990 rpm speed.

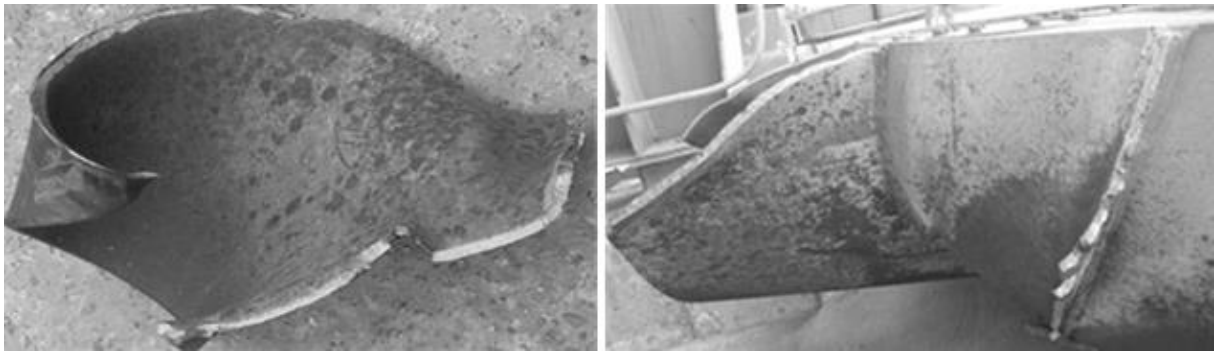

Figure 4. Example of fracture failure (left) and an example of breaking the blades from the root (right side).

Figure 5. View of corrective fan with manufacturer recommendation.

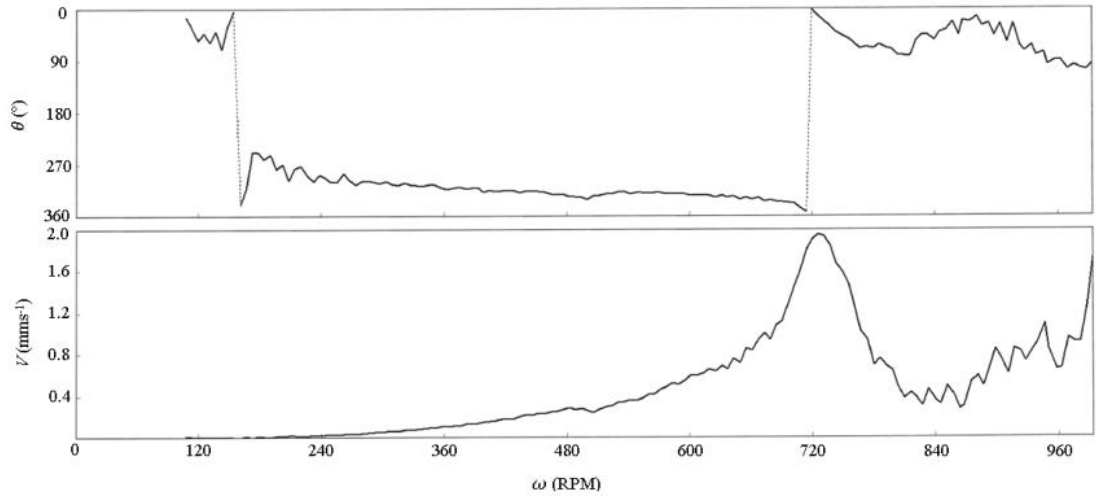

Figure 6. Coast down diagram for analysis fan (based on experimental test).

Table 3. Manufacturer's catalog data of volumetric flow rate at full load (manufacturer's instructions).

fuel	Load percentage	Entrance volumetric flow rate(m^3/s)	Density of smoke(kg/m^3)
mazzot	100	205	0.702
gas	100	211.1	0.627

At fan inlet to control discharge and fan pressure, control damper is used which controls the flow rate by opening and closing. At the input of a fan, a device for making the flow laminar is installed. Also in the fan outlet there are a number of stationary blades for direct flow to the chimney. Fan with creating vacuum at the entrance,

puts the combustion chamber under vacuum. The vacuum mentioned is about 5 millimeters of water column. In the outlet, after the blades, a diffuser has been installed to increase the pressure of the smoke. The details are shown in Fig. 7.

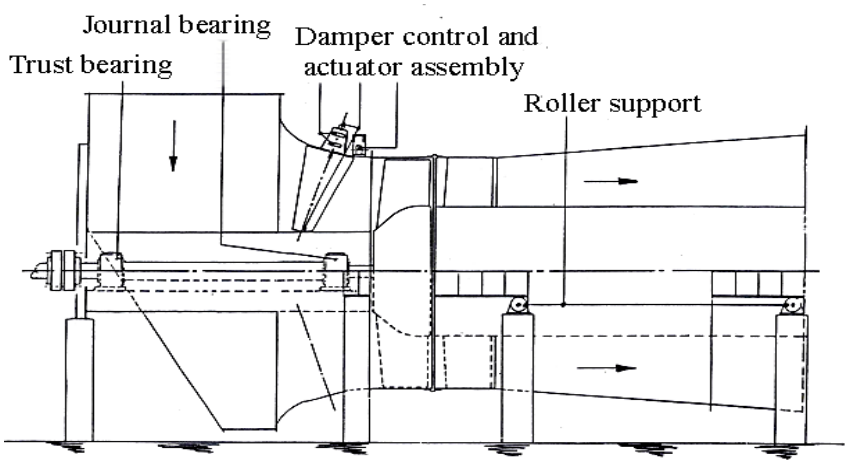

Figure 7. Different parts of the fan and the direction of smoke flow (manufacturer's instructions).

Equations

The governing equations change according to the simulation conditions. Given the hypothesized issues in this study time-dependent parameters in the equations are reduced, and Equations obtained are (Afzalimehr, 2012):

$$Conservation\ of\ \ mass\ :\nabla.(\rho\vec{V})=0 \tag{1}$$

$$X\ -momentum:\nabla.(\rho u\vec{V})=-\frac{\partial P}{\partial x}+\frac{\partial \tau_{xx}}{\partial x}+\frac{\partial \tau_{yx}}{\partial y}+\frac{\partial \tau_{zx}}{\partial z} \tag{2}$$

$$y-momentum:\nabla.(\rho v\vec{V})=-\frac{\partial P}{\partial y}+\frac{\partial \tau_{xy}}{\partial y}+\frac{\partial \tau_{yy}}{\partial y}+\frac{\partial \tau_{zy}}{\partial z}+\rho g \tag{3}$$

$$z-momentum:\nabla.(\rho w\vec{V})=-\frac{\partial P}{\partial z}+\frac{\partial \tau_{xz}}{\partial x}+\frac{\partial \tau_{yz}}{\partial y}+\frac{\partial \tau_{zz}}{\partial z} \tag{4}$$

Given the turbulence of fluid flow in this research, turbulence effects are calculated using turbulence model. Choosing the turbulent model in simulation is very important and in this study, the turbulence model for the stable state of the model equations is (Hoffmann & Chiang, 1989):

$$\mu_t=\rho f_{v1}\nu \tag{5}$$

The coefficients are defined as follows:

$$C_{w1}=\frac{C_{b1}}{K^2}+\frac{(1+C_{b2})}{\sigma_\nu} \tag{6}$$

$$C_{b1}=0.13355, C_{b2}=0.622, C_{\nu 1}=7.1$$
$$C_{w2}=0.3, C_{w3}=2.0, K=0.418, \sigma_\nu=2/3 \tag{7}$$

The standard K-ε model is a semi-experimental model for kinetic energy turbulence and loss rate ε based on the transport equations. This model is a turbulence model with two equations and one of the most powerful turbulence models for engineering issues. Being Powerful, economical and have acceptable accuracy in a wide

range of turbulence flows are causes that this model has become popular in industrial matters. For the K-ε stable state, the following transition equations are obtained (Hoffmann & Chiang, 1989):

$$\frac{\partial}{\partial x_i}(\rho k u_i) = \frac{\partial}{\partial x_j}[(\mu + \frac{\mu_t}{\sigma_k})\frac{\partial k}{\partial x_j}] + G_k + G_b - \rho\varepsilon + S_k \tag{8}$$

$$\frac{\partial}{\partial x_i}(\rho \varepsilon u_i) = \frac{\partial}{\partial x_j}[(\mu + \frac{\mu_t}{\sigma_\varepsilon})\frac{\partial \varepsilon}{\partial x_j}] + C_{1\varepsilon}\frac{\varepsilon}{k}(G_k + G_{3\varepsilon}G_b) - C_{2\varepsilon}\rho\frac{\varepsilon^2}{k} + S_\varepsilon \tag{9}$$

The model constants have the following values:

$$C_{1\varepsilon} = 1.44, C_{2\varepsilon} = 1.92, C_\mu = 0.09, \sigma_k = 1.0, \sigma_\varepsilon = 1.3 \tag{10}$$

The main difference between the real K-ε model and the standard is the existence of a new formula for turbulent viscosity in the real model and represents the rate of loss of different transfer equations. In the real K-ε model for a stable state ε, following equation base on transfer equations are obtained:

$$\frac{\partial}{\partial x_j}(\rho \varepsilon u_j) = \frac{\partial}{\partial x_j}[(\mu + \frac{\mu_t}{\sigma_\varepsilon})\frac{\partial \varepsilon}{\partial x_j}] + \rho C_1 S\varepsilon + C_{1\varepsilon}\frac{\varepsilon}{K}C_{3\varepsilon}G_b - C_2\rho\frac{\varepsilon^2}{K + \sqrt{\varepsilon\nu}} + S_\varepsilon \tag{11}$$

The value of the constants of the model is as follows:

$$C_{1\varepsilon} = 1.44, C_{2\varepsilon} = 1.9, \sigma_k = 1.0, \sigma_\varepsilon = 1.2 \tag{12}$$

Simulating Method

In general, the flow between the blades of a turbo-machinery, for various reasons, including the occurrence of secondary flow, shock and separation phenomena, can be a complex and three-dimensional flow. Today, for the analysis of such complex flows, specialized turbo-machinery software is used (Dehghanisanich, 2013). The general steps of a numerical simulation are shown in Fig. 8. The first step for using of CFD soft wares is modeling the Intended issue in modeling soft wares like CATIA. Meshing and creating the boundary conditions are else steps for simulating in CFD software. The results should be validated through laboratory data or research papers or experimental tests. And then, for other functional states, we can use the computational fluid dynamics results with confidence (Dehghanisanich, 2013). Modeling the whole structure of the fan and its duct together with the inlet damper and the outlet damper, requires a high volume of computing, a strong server and a long time for convergence, so simplification has been done to simulate.

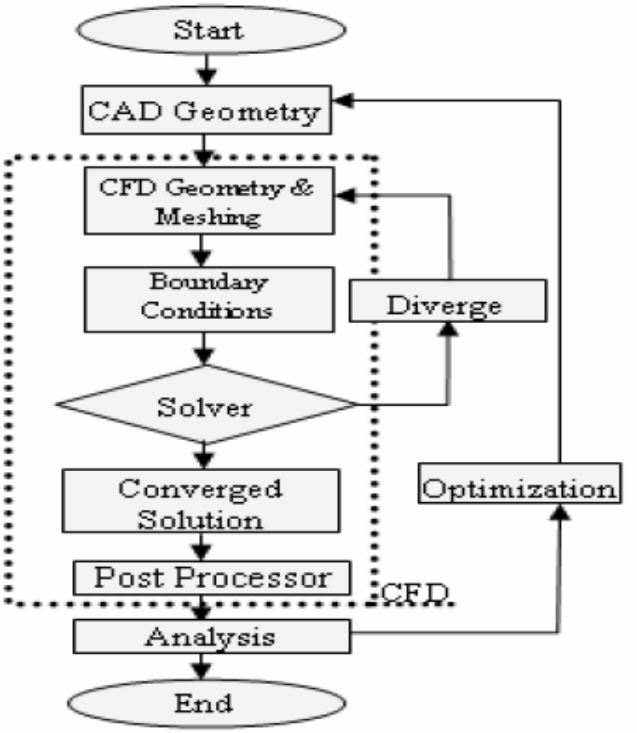

Figure 8. Modeling and optimization flowchart in general (Yossof Soleyman et al., 2002).

During the simulation, the input damper is assumed to be completely open and the flow is laminar and without turbulence at inlet of fan. Since the fluid is smoke, its density is determined and assumes that the fan receives the fluid from environment and delivers it to the environment. Since the pressure variations in the fans are low, the assumption is reasonable and the fan discharge is analyzed.

Fan is modeled in "CATIA" software and in the "GAMBIT" software hub and the inlet and outlet, and the fluid passage area are specified. Then the geometry of fan is gotten by "ANSYS WORKBENCH" software and the fluid passage is detected and meshed. Then it has been analyzed in the "FLUENT" software, which is available in the package of "ANSYS WORKBENCH". In this simulation, the condition of pressure has been used for the input and output boundaries. The relative pressure is the same for both and it is equal the atmospheric pressure of installation place.

A rotating reference algorithm is used to model rotor rotation. For rotor rotation, the moving boundary condition with zero rotational speed rather Than reference is used. Shell boundary condition is wall condition with non-slip condition. During the simulation, the standard K-ε method has been used. In this study due to irregular geometry, especially when supports are added to fan blades, Triangular-pyramid mesh is used. Three different sizes of the mesh, big, medium and fine mesh have been investigated. But since the number of meshes increased from the second manner (medium meshes) to the third (fine meshes), and there was not much difference in the solution, then Simulation on the second manner is independent of mesh numbers. Table 4 shows the numbers of the meshes and the answers to each of the mesh manners. This number of cells is related to without any support geometry mode. But in the case with the supports, the geometry becomes more complex and since the purpose of this simulation is to study the effects of these supports gridding close to these supports is fine and sometimes the number of meshes reaches six million cells.

Table 4. Appropriate mesh survey.

Meshing manner	Number of cells	Mass flow rate (kg/s)
First manner (big meshes)	186354	139.27385
Second manner (medium meshes)	299788	141.63126
Third manner (fine meshes)	487357	142.14837

The results of various simulations

First simulation was performed for the initial state of the fan without any supports. By checking the flow on the above mentioned fan, the flow rate was 141.6 (kg/s) and due to the smoke density in the fuel oil (mazzot), it is 201.75 (m^3/s). This means that in simulating, the flow rate has less than 2% error rather than information in manufacturer catalogue of fan which is shown in table (5). Figure 9 shows the convergence diagram of the solution. In Figure 10, the vacuum side and the pressure side on fan blades and streamlines through them is shown. The fan rotates in the direction of x in figure 10.

Table 5. Simulation verification.

condition	Mass flow rate (kg/s)
simulation	141.63126
Catalogue of fan	143.91
Percentage of error	1.6 %

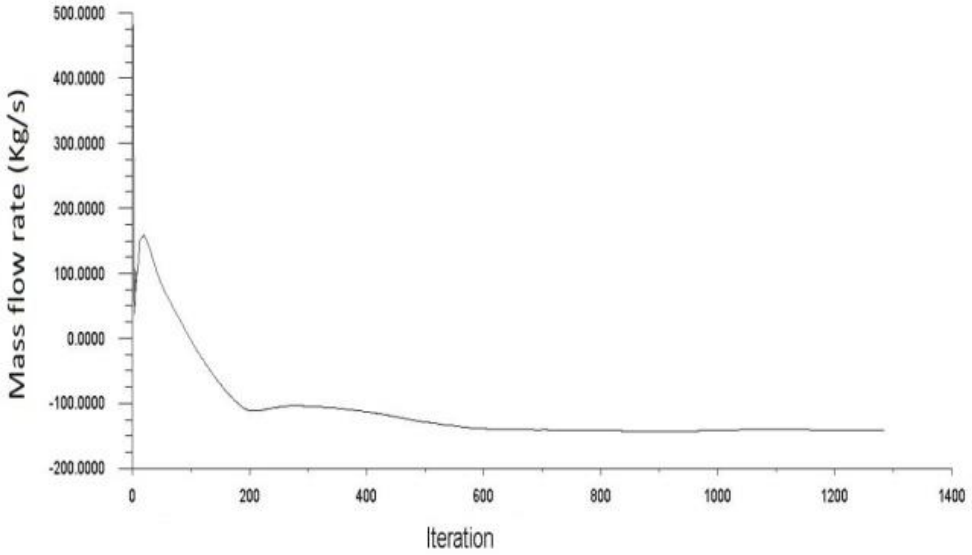

Figure 9. Flow convergence graph for Analysis without any support.

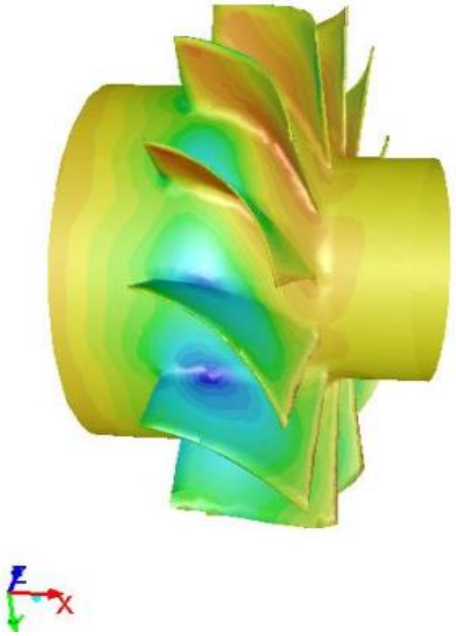

Figure 10. Vacuum side and pressure side of fan blades.

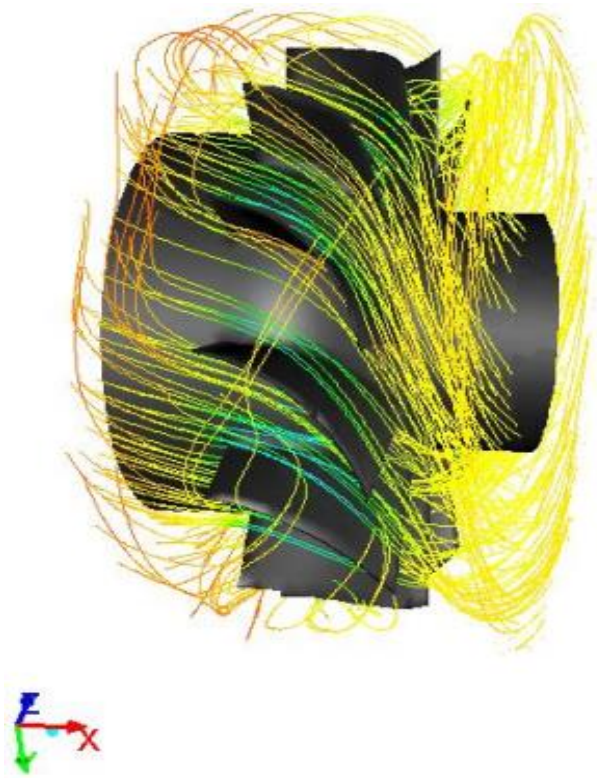

Figure 11. Streamlines in fan analysis.

Because it is considered that for increasing the strength of the blades, add them supports, therefore, other states were considered, which are shown in Figs. (12) to (14). Figure 12 shows the German manufacturer's suggestion. Figures (13) and (14) consider other suggestions as new designs.

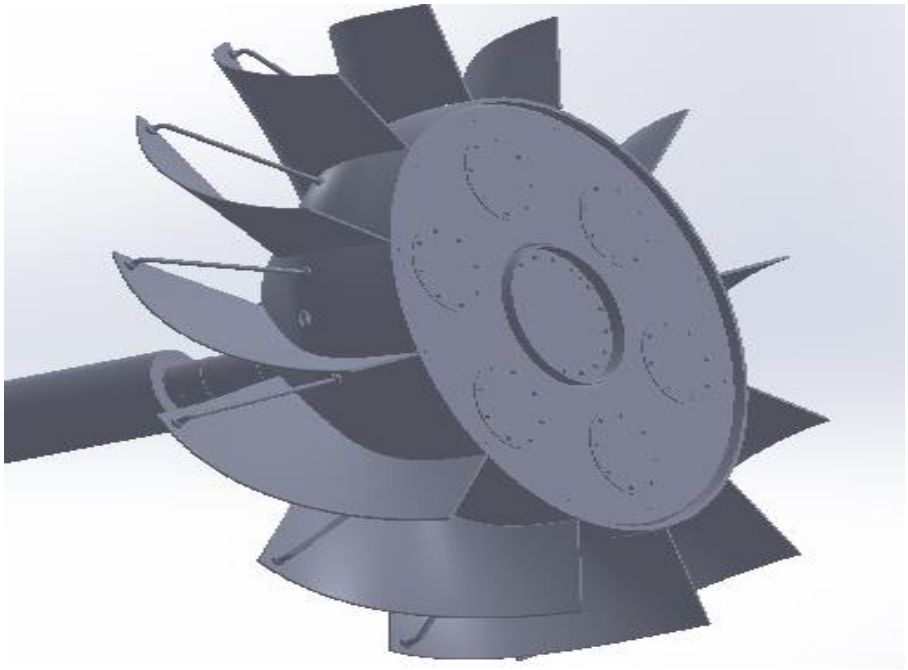

Figure 12. The geometry of the fan which there are some supports like cane that they are welded to hub and blades.

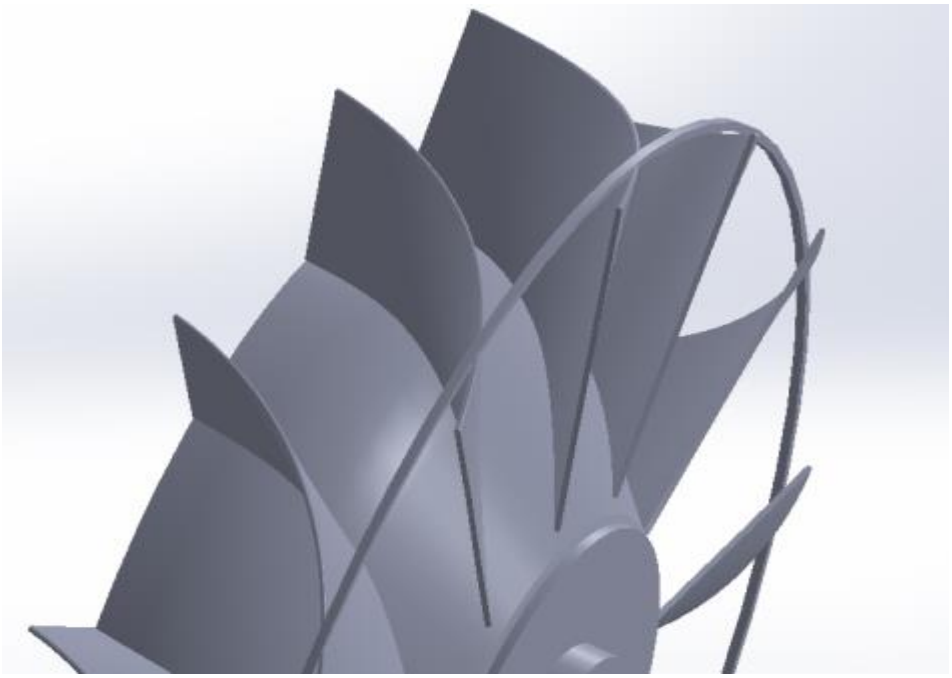

Figure 13. The geometry of the fan, when it is surrounded and welded by a belt ring (rectangular cross section) or a bar ring (circular cross section) to the blades.

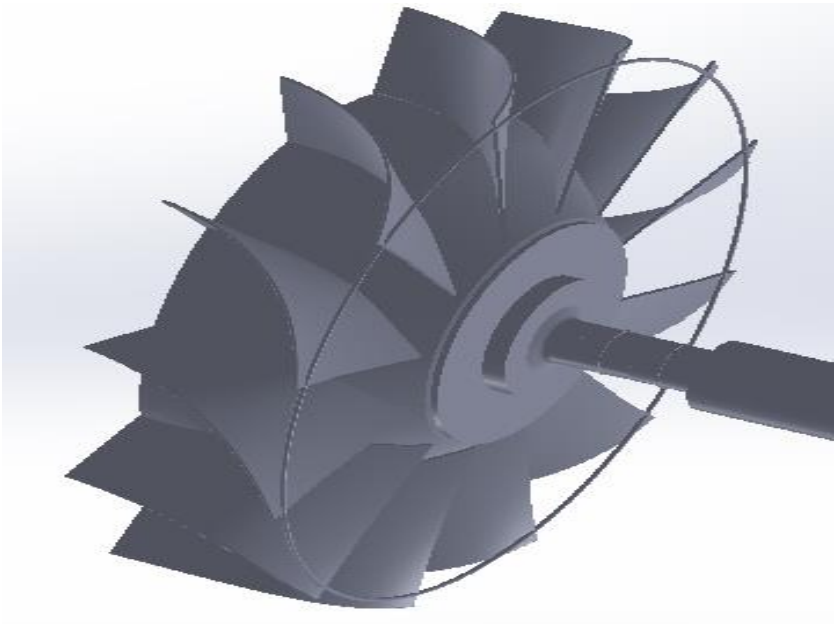

Figure 14. Fan geometry in the case of a bar ring (circular cross section) or a belt ring (rectangular cross section) welded to fan's brow.

Fig. 13 comprises a circular cross-section or a rectangular cross-section support connected to the circumference of the blades. They are named in the order of the "bar ring around the blade" and "belt ring around the blades". Figure (14) comprises a circular cross-section or a rectangular cross section support in brow of blades.

Tables (6) to (11) show the results of simulation at both fan speeds.

Also, the figure (15) and figure (16) show the flow streamlines for the cane like supports and the bar ring around the blades.

Table 6. Comparison the flow rates at 740 rpm.

Various scenarios in the 740 rpm	*Mass flow rate(kg/s)*
The main mode, without any support	105.73076
Bar ring around the blades	76.821947
Belt ring around the blades	98.208905
Bar ring in blades brow	86.761314
Belt ring in blades brow	104.34645
Blades with separate support (manufacturer suggestion)	67.893703

Table 7. Comparison of torsional moment at 740 rpm.

Various scenarios in the 740 rpm	*Torque(N.M)*
The main mode, without any support	6858.1509
Bar ring around the blades	4272.303
Belt ring around the blades	6188.8153
Bar ring in blades brow	4928.5286
Belt ring in blades brow	6777.7457
Blades with separate support (manufacturer suggestion)	3804.2292

Table 8. Comparison of the trust force at 740 rpm.

Various scenarios in the 740 rpm	*Trust force(N)*
The main mode, without any support	5776.4113
Bar ring around the blades	3188.694
Belt ring around the blades	5014.4306
Bar ring in blades brow	3952.0015
Belt ring in blades brow	5625.4755
Blades with separate support (manufacturer suggestion)	2845.7229

Table 9. Comparison the flow rates at 990 rpm.

Various scenarios in the 990 rpm	*Mass flow rate(kg/s)*
The main mode, without any support	141.63126
Bar ring around the blades	107.42166
Belt ring around the blades	129.36852
Bar ring in blades brow	114.6151
Belt ring in blades brow	136.58531
Blades with separate support (manufacturer suggestion)	89.30028

Table 10. Comparison of torsional moment at 990 rpm.

Various scenarios in the 990 rpm	*Torque(N.M)*
The main mode, without any support	12266.121
Bar ring around the blades	7950.8454
Belt ring around the blades	10939.531
Bar ring in blades brow	9296.8746
Belt ring in blades brow	11993.026
Blades with separate support (manufacturer suggestion)	6737.278

Table 11. Comparison of the trust force at 990 rpm.

Various scenarios in the 990 rpm	*Trust force(N)*
The main mode, without any support	10337.388
Bar ring around the blades	6018.2366
Belt ring around the blades	8883.9157
Bar ring in blades brow	8089.3733
Belt ring in blades brow	9804.6147
Blades with separate support (manufacturer suggestion)	4905.5163

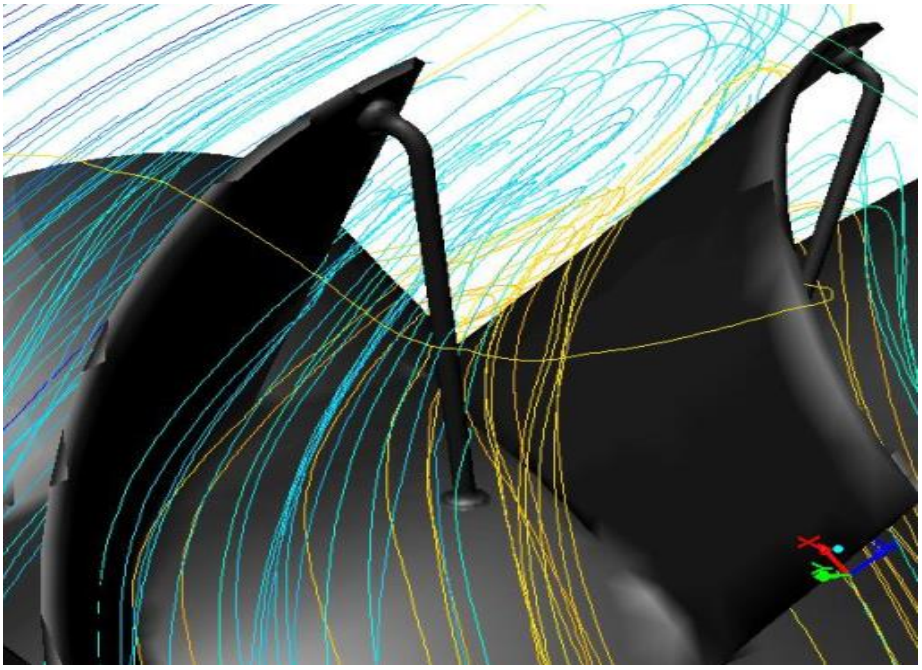

Figure 15. Streamlines for fan with cane like supports.

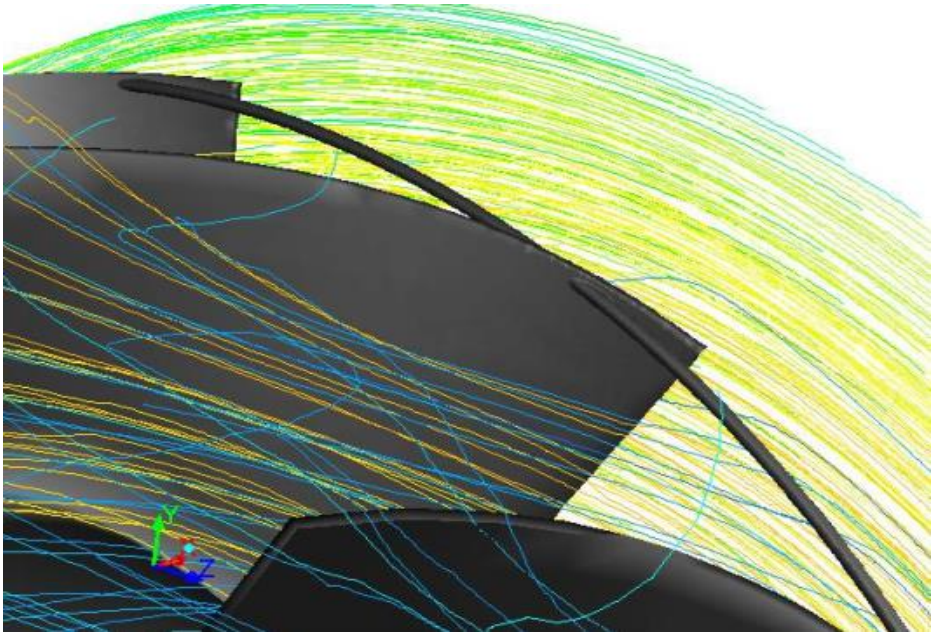

Figure 16. Streamlines for a state in which a bar surrounded and welded around the blades.

Conclusion

It is clear from Tables 6 and 9 that the flow rate of the fan decreases with adding support. Although the manufacturer's recommendation (support like cane in fig. 15) is more durable than the rest of considered scenarios but it is worst manner between other considered scenarios in term of flow rate. This negative impact is so high and flow rate is 37% lower than normal manner (without any support on blades) at 990 rpm. Even the flow rate at 990 rpm with cane like support is lower than flow rate at 740 rpm without any supports. The boiler's fans are designed to provide boiler ventilation in their first speed but fan with cane like supports has forced operators to operate fans at second speed (990 rpm). As noted, all supports have its own negative effect but belt ring around the blades has the best result between them that has lower than 3% negative effect.

Tables 7 and 8 as well as 10 and 11, at both fan speeds, show trust forces and fan torques. Although there is no information available for verifying them but the process of change indicates that increased flow through the fan will increase these forces. Of course, the process of these changes is acceptable and reasonable.

It should be noted that in terms of execution, adding different supports requires consideration of welding issues, economic issues, heat treatment, and Non-destructive testing.

References

Afzalimehr, H. (2012). Fluid Mechanics Study through Note, Problem and Test (In Persian), Arkan Danesh Publishing. [Publisher]

Akbari, M. R., & dadkhah, M. (2017). An Introduction to Gas Ejector Design, Kanoon pajoohesh publishing. [Publisher]

ASME Fans standard, (2008). PTC- 11.

Dehghanisanich, M. A. (2013). Numerical Simulation with Fluent 6.3(In Persian), Naghoos Publishing. [Publisher]

EL-Wakill, M .M. (1985). Power Plant Technology, McGraw-Hill. [Publisher]

Hadizade, D. (2015). Complete design and implementation of mechanical Equipment, Noavar publishing. [Publisher]

Hoffmann, K. A., & Chiang, S. T. (1989). Computational Fluid Dynamics for Engineers Vol. 2, Publication of Engineering Education System", Wichita, Kansas, USA. [Google Scholar] [Publisher]

McPherson, M. J. (1993). Subsurface Ventilation Engineering. [Publisher]

Tabatabaee, M. (2003). Building Facilities Calculations (In Persian), Roozbehan Publishing, Iran. [Publisher]

U.S Department of energy, Improving Fan System Performance (a sourcebook for industry) [Publisher]

Yossef Solaiman, M., & Bahari Azraai, S., & Mokhtar Wan Abdullah, W. (2002). CFD Modeling of air flow distribution.